

Transport through a quantum wire with a side quantum-dot array

P. A. Orellana,¹ F. Domínguez-Adame,² I. Gómez,² and M. L. Ladrón de Guevara³

¹*Departamento de Física, Universidad Católica del Norte, Casilla 1280, Antofagasta, Chile*

²*Departamento de Física de Materiales, Universidad Complutense, E-28040 Madrid, Spain*

³*Departamento de Física, P. Universidad Católica de Chile, Casilla 306, Santiago 22, Chile.*

(Dated: October 31, 2018)

A noninteracting quantum-dot array side-coupled to a quantum wire is studied. Transport through the quantum wire is investigated by using a noninteracting Anderson tunneling Hamiltonian. The conductance at zero temperature develops an oscillating band with resonances and antiresonances due to constructive and destructive interference in the ballistic channel, respectively. Moreover, we have found an odd-even parity in the system, whose conductance vanishes for an odd number of quantum dots while becomes $2e^2/h$ for an even number. We established an explicit relation between this odd-even parity, and the positions of the resonances and antiresonances of the conductivity with the spectrum of the isolated QD array

PACS numbers: PACS number(s): 73.21.La; 73.63.Kv; 85.35.Be

I. INTRODUCTION

Recent progress in nanofabrication of quantum devices enables to study electron transport through quantum dots (QDs) in a very controllable way.^{1,2} QDs are very promising systems due to their physical properties as well as their potential application in electronic devices. These structures are small semiconductor or metal structures in which electrons are confined in all spatial dimensions. As a consequence, discreteness of energy and charge arise. For this reason QDs are often referred as *artificial atoms*. In contrast to real atoms, different regimes can be studied by continuously changing the applied external potential.

If the single QDs is referred as *artificial atoms* a QD array can be considered as *artificial molecule* or *artificial crystal*.^{3,4,5} Latest advances in nanotechnology make it possible to fabricate QD arrays. In linear QD arrays leads are attached to their ends and the current through them is measured while external parameters such as a gated voltage, magnetic field, and temperature are varied. In resonant tunneling regime, the electronic transport through QD array becomes sensitive to precise matching of the electron levels in the dots that can be controlled experimentally. For other hand, a linear QD array can be seen as an one dimensional chain of sites. This type of chain coupled to the continuum states shows an even-odd parity effect in the conductance when the Fermi energy is localized in the center of the energy band.^{6,7} The conductance is $2e^2/h$ for odd samples and is smaller for even parity.^{6,7}

The aim of this work is to study theoretically the transport properties of an alternative configuration of a side-coupled QD array attached to a perfect quantum wire (QW). In this case the QD array acts as scattering center for transmission through the QW. This configuration can be regarded as a quantum wave guide with side-stub structures, similar to those reported in Refs. 8,9,10. In contrast to the embedded QD array, the transmission through the side-coupled QD array consists of the interference between the ballistic channel and the resonant

channels from the QD array. For a uniform side QD array, we found that the system develops an oscillating band with resonances (perfect transmission) and antiresonances (perfect reflection). In addition, we found an odd-even parity of the number of QDs in the array, namely perfect transmission takes place if this number is even ($G = 2e^2/h$) but perfect reflection arises for an odd number ($G = 0$). This result is opposed to that found in embedded QD arrays.^{6,7} We established an explicit relation between this odd-even parity, and the positions of the resonances and antiresonances of the conductivity with the spectrum of the isolated QD array.

II. MODEL

Let us consider a QW with a side-coupled QD array. The array consists of N QDs connected in a series by tunnel coupling, as shown in Fig. 1. The system is modeled by using a noninteracting Anderson tunneling Hamiltonian⁵ that can be written as

$$H = H_{\text{QW}} + H_{\text{QD}}^N + H_{\text{QD-QW}}, \quad (1)$$

with

$$\begin{aligned} H_{\text{QW}} &= v \sum_{i \neq j} c_i^\dagger c_j, \\ H_{\text{QD}}^N &= \sum_{l=1}^N \varepsilon_l d_l^\dagger d_l + \sum_{l=1}^{N-1} (V_{l,l+1} d_l^\dagger d_{l+1} + \text{h.c.}), \\ H_{\text{QD-QW}} &= V_0 (d_1^\dagger c_0 + c_0^\dagger d_1). \end{aligned} \quad (2)$$

The operator c_i^\dagger creates an electron at site i , v is the hopping in the QW, ε_l is the energy level of the dot l and $V_{l,l+1}$ is the tunneling coupling between l th and $(l+1)$ th QD. Here H_{QW} corresponds to the free-particle Hamiltonian on a lattice with spacing d and whose eigenfunctions

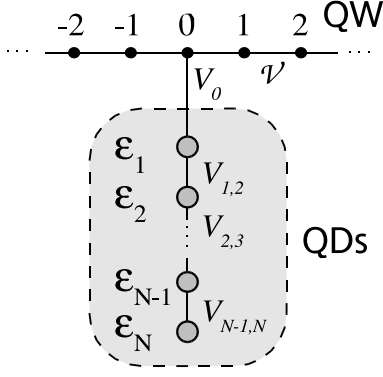


FIG. 1: Side-coupled quantum dot array attached to a perfect quantum wire.

are expressed as Bloch solutions

$$|k\rangle = \sum_{j=-\infty}^{\infty} e^{ikdj} |j\rangle, \quad (3)$$

where $|k\rangle$ is the momentum eigenstate and $|j\rangle$ is a Wannier state localized at site j . The dispersion relation associated with these Bloch states reads

$$\varepsilon = 2v \cos(kd). \quad (4)$$

Consequently, the Hamiltonian supports an energy band from $-2v$ to $+2v$ and the first Brillouin zone expands the interval $[-\pi/d, \pi/d]$.

The stationary states of the entire Hamiltonian H can be written as

$$|\psi_k\rangle = \sum_{j=-\infty}^{\infty} a_j^k |j\rangle + \sum_{l=1}^N b_l^k |l\rangle, \quad (5)$$

where the coefficient a_j^k (b_l^k) is the probability amplitude to find the electron in the site j of the QW (l of the array) in the state k , namely

$$a_j^k = \langle j | \psi_k \rangle, \quad b_l^k = \langle l | \psi_k \rangle. \quad (6)$$

The amplitudes a_j^k obey the following linear difference equations

$$\begin{aligned} \varepsilon a_j^k &= v(a_{j-1}^k + a_{j+1}^k) + V_0 b_1^k \delta_{j0}, \\ \varepsilon b_1^k &= \varepsilon_1 b_1^k + V_{1,2} b_2^k + V_0 a_0^k, \\ \varepsilon b_l^k &= \varepsilon_l b_l^k + V_{l,l-1} b_{l-1}^k + V_{l,l+1} b_{l+1}^k, \quad l \neq 1, N, \\ \varepsilon b_N^k &= \varepsilon_N b_N^k + V_{N,N-1} b_{N-1}^k. \end{aligned} \quad (7)$$

Iterating backwards the equation for b_N^k we can express the amplitude b_1^k in terms of a_0^k as a continued fraction

$$b_1^k = \frac{V_0 a_0^k}{\varepsilon - \varepsilon_1 - \frac{V_{1,2}^2}{\varepsilon - \varepsilon_2 - \dots \frac{V_{N-1,N}^2}{\varepsilon - \varepsilon_{N-1} - \frac{V_{N,N-1}^2}{\varepsilon - \varepsilon_N}}}}. \quad (8)$$

Therefore the equation for a_0^k can be cast in the form

$$\varepsilon a_0^k = v(a_{-1}^k + a_1^k) + V_0^2 / Q_N a_0^k, \quad (9)$$

where Q_N is the continued fraction

$$Q_N = \varepsilon - \varepsilon_1 - \frac{V_{1,2}^2}{\varepsilon - \varepsilon_2 - \dots \frac{V_{N-1,N}^2}{\varepsilon - \varepsilon_{N-1} - \frac{V_{N,N-1}^2}{\varepsilon - \varepsilon_N}}}. \quad (10)$$

In order to study the solutions of the equations (7) we assume that the electrons are described by a plane wave incident from the far left with unity amplitude and a reflection amplitude r and at the far right by a transmission amplitude t . Taking this to be the solution we can write,

$$a_j^k = e^{ikdj} + r e^{-ikdj}, \quad j < 0, \quad (11)$$

$$a_j^k = t e^{ikdj}, \quad j > 1. \quad (12)$$

The solution of the equations for the a_j^k 's can be then obtained iteratively from right to left. For a given transmission amplitude, the associated incident and reflection amplitudes may be determined by matching the iterated function to the proper plane wave at the far left. The transmission probability is given by $T = |t|^2$ and is obtained from the iterative procedure described above. In equilibrium we solve the equation for t and r and we get the following expressions

$$t = \frac{2iv \sin(kd)}{2iv \sin(kd) - V_0^2 / Q_N} = \frac{Q_N}{Q_N + i\Gamma}, \quad (13a)$$

$$r = -\frac{V_0^2 / Q_N}{2iv \sin(kd) - V_0^2 / Q_N} = \frac{i\Gamma}{Q_N + i\Gamma}, \quad (13b)$$

where $\Gamma(\varepsilon) \equiv V_0^2 / 2v \sin(kd)$ can be regarded as the level broadening. Notice that the level broadening can be fairly well approximated by $\Gamma \simeq V_0^2 / 2v$ close to the center of the band.

The experimentally accessible quantity is the linear conductance G which is related to the transmission coefficient T at the Fermi energy by the one-channel Landauer formula at zero temperature

$$G = \frac{2e^2}{h} T = \frac{2e^2}{h} \frac{Q_N^2}{Q_N^2 + \Gamma^2}. \quad (14)$$

It is worth mentioning that the energy levels (zeroes of Q_N) depend only on the hopping in the QD array ($V_{n-1,n}$) while Γ is only function of V_0^2 / v . Consequently, both magnitudes can be controlled independently in an actual experiment. This is one of the main advantages of the present setup.

III. RESULTS

A. Short QD array

Closed expressions for the transmission and reflection coefficients can be readily obtained when the number of

QDs in the array is small. For $N = 1$, $Q_1 = \varepsilon - \varepsilon_1$ and then we arrive at

$$\begin{aligned} T(\varepsilon) &= \frac{(\varepsilon - \varepsilon_1)^2}{(\varepsilon - \varepsilon_1)^2 + \Gamma^2}, \\ R(\varepsilon) &= \frac{\Gamma^2}{(\varepsilon - \varepsilon_1)^2 + \Gamma^2}. \end{aligned} \quad (15)$$

The system has an antiresonance at $\varepsilon = \varepsilon_1$. The transmission and the reflection probability are zero and one, respectively. For $N = 2$, the transmission and reflection coefficients are given by

$$\begin{aligned} T(\varepsilon) &= \frac{[(\varepsilon - \varepsilon_1)(\varepsilon - \varepsilon_2) - V_c^2]^2}{[(\varepsilon - \varepsilon_1)(\varepsilon - \varepsilon_2) - V_c^2]^2 + (\varepsilon - \varepsilon_2)^2 \Gamma^2}, \\ R(\varepsilon) &= \frac{(\varepsilon - \varepsilon_2)^2 \Gamma^2}{[(\varepsilon - \varepsilon_1)(\varepsilon - \varepsilon_2) - V_c^2]^2 + (\varepsilon - \varepsilon_2)^2 \Gamma^2}, \end{aligned} \quad (16)$$

where $V_{1,2} \equiv V_c$. Therefore, the system presents one resonance in $\varepsilon - \varepsilon_2$ and bonding and antibonding antiresonances at energies

$$\varepsilon = \frac{1}{2}(\varepsilon_1 + \varepsilon_2) \pm \frac{1}{2}\sqrt{(\varepsilon_1 - \varepsilon_2)^2 + 4V_c^2}.$$

The system with $N = 3$ side-coupled QDs shows particularly simple solution for the case $V_{1,2} = V_{2,3} \equiv V_c$,

$$\begin{aligned} T(\varepsilon) &= \frac{[(\varepsilon - \varepsilon_1)(\varepsilon - \varepsilon_2)(\varepsilon - \varepsilon_3) - V_c^2((\varepsilon - \varepsilon_1) + (\varepsilon - \varepsilon_3))]^2}{[(\varepsilon - \varepsilon_1)(\varepsilon - \varepsilon_2)(\varepsilon - \varepsilon_3) - V_c^2((\varepsilon - \varepsilon_1) + (\varepsilon - \varepsilon_3))]^2 + [(\varepsilon - \varepsilon_2)(\varepsilon - \varepsilon_3) - V_c^2]^2 \Gamma^2}, \\ R(\varepsilon) &= \frac{[(\varepsilon - \varepsilon_2)(\varepsilon - \varepsilon_3) - V_c^2]^2 \Gamma^2}{[(\varepsilon - \varepsilon_1)(\varepsilon - \varepsilon_2)(\varepsilon - \varepsilon_3) - V_c^2((\varepsilon - \varepsilon_1) + (\varepsilon - \varepsilon_3))]^2 + [(\varepsilon - \varepsilon_2)(\varepsilon - \varepsilon_3) - V_c^2]^2 \Gamma^2}. \end{aligned} \quad (17)$$

Clearly for the case with $\varepsilon_1 = \varepsilon_2 = \varepsilon_3$, the system shows three antiresonances at $\varepsilon = \varepsilon_1$ and $\varepsilon = \varepsilon_1 \pm \sqrt{2}V_c$ and two resonances at $\varepsilon = \varepsilon_1 \pm V_c$.

Figure 2 shows the conductance as a function of the Fermi energy of the incident electron for $\varepsilon_i = 0$ ($i = 1, \dots, N$) and $V_c = \Gamma$. There exists only one narrow antiresonance in the case of $N = 1$ QD, and bonding and antibonding antiresonances and one resonance in zero are clearly revealed for $N = 2$. In addition, bonding and antibonding resonances and zero, bonding and antibonding antiresonances arise when $N = 3$.

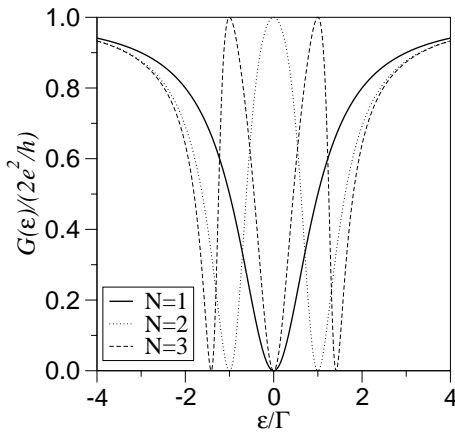


FIG. 2: Conductance, in units of $2e^2/h$, versus Fermi energy, in units of the Γ , for the case of the one, two and three QD array with $V_c = \Gamma$.

B. Long QD array

When the number N of attached QDs is large, we must rely on numerical calculations. For sake of simplicity we consider a uniform quantum dot array $V_{l-1,l} \equiv V_c$ and $\varepsilon_l = \varepsilon_0$. The continued fraction Q_N in Eq. (10) is written as $Q_N = (\varepsilon - \varepsilon_0)x_N$, where x_N satisfies the following recursive equation,

$$x_N = 1 - \frac{\alpha}{x_{N-1}}, \quad N = 1, 2, 3, \dots \quad (18)$$

with $x_1 = 1$ and $\alpha \equiv V_c^2/(\varepsilon - \varepsilon_0)^2$ for $\varepsilon \neq \varepsilon_0$.

For N large the antiresonance appearing in Fig. 2 for $N = 1$ evolves as a fast oscillation band. As the number of QDs N increases, this narrow antiresonance splits into N antiresonances and $N - 1$ resonances, as seen in the upper panel of Fig. 3 for $V_c = \Gamma$ and $\varepsilon_0 = 0$. On further increasing N , the antiresonances never merge into a single stop-band, as one would naively expect. In fact, it is not difficult to demonstrate that $Q_N = D_N/D_{N-1}$, where $D_N = \det(H_{QD}^N - \varepsilon I)$. The transmission coefficient can be written as

$$T = \frac{D_N^2}{D_N^2 + \Gamma^2 D_{N-1}^2}. \quad (19)$$

Thus, transmission vanishes in the spectrum of H_{QD}^N and becomes unity in the spectrum of the H_{QD}^{N-1} . Therefore the conductance show N antiresonances and $N - 1$ resonances, as we see in Figs. 1 and 2. This statement is

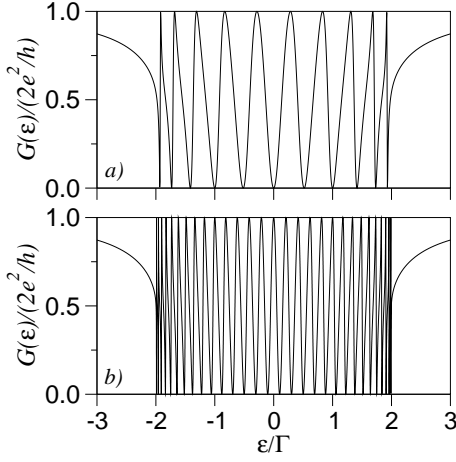


FIG. 3: Conductance, in units of $2e^2/h$, versus Fermi energy, in units of Γ , for a) $N = 11$ and b) $N = 30$ QD array with $V_c = \Gamma$ and $\varepsilon_0 = 0$.

further confirmed by plotting the full width at half minimum of the antiresonances, Δ , as a function of energy, as shown in Fig. 4 for different values of N .

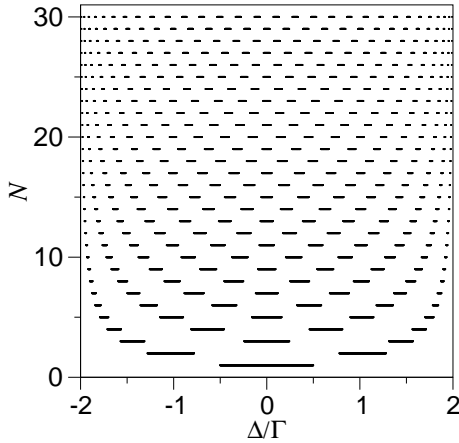


FIG. 4: Full width at half minimum of the antiresonances Δ for different values of N and $V_c = \Gamma$. Each segment joints the two energies for which conductance becomes e^2/h on every antiresonance.

C. Odd-Even Parity

Here we consider the case when the Fermi energy is pinned at the value of the energy level of the quantum dot. From equation (7) is straightforward to prove the existence of an odd-even parity when $\varepsilon_l = \varepsilon_0$,

$$\begin{aligned} G &= 0, & N &\text{ odd,} \\ G &= \frac{2e^2}{h}, & N &\text{ even,} \end{aligned} \quad (20)$$

as it can be readily checked in Figs. 1 and 2. This result also holds for QD arrays with off-diagonal disorder.

This odd-even parity is opposed to the case of an embedded quantum array, where perfect transmission takes place for odd parity.^{6,7} This property arises from the fact that energy level of the of the QDs ε_0 is always in the electronic spectrum of the isolated QD array, provided the number of the QDs is odd. It is straightforward to demonstrate this statement from the fact D_N satisfies the following recursive equation,

$$D_N = (\varepsilon - \varepsilon_0)D_{N-1} - V_{N-1,N}^2 D_{N-2}, \quad N = 3, 4, 5 \dots \quad (21)$$

with $D_1 = \varepsilon - \varepsilon_0$ and $D_2 = (\varepsilon - \varepsilon_0)^2 - V_{1,2}^2$. It is clear from Eq. (21) that D_N is zero at $\varepsilon = \varepsilon_0$ if N is odd. Therefore ε_0 is eigenvalue of H_{QD}^N and then from equation (19) we obtain that at $\varepsilon = \varepsilon_0$, $T = 0$ (perfect reflection) if N is odd and $T = 1$ (perfect transmission) for even N .

D. Infinite QD array

To understand the origin of the fast oscillations of the conductance as a function of the Fermi energy (Fig. 3), we now consider the limiting case $N \rightarrow \infty$. Thus, we are faced to a one-dimensional map (18). This map has two fixed points at¹¹

$$x_{\pm}^* = \frac{1}{2} \left(1 \pm \sqrt{1 - 4\alpha} \right), \quad (22)$$

when $\alpha < 1/4$, namely $|\varepsilon - \varepsilon_0| > 2V_c$. The conductance for $N \rightarrow \infty$ is,

$$G_{\infty} = \frac{2e^2}{h} \frac{(|\varepsilon - \varepsilon_0| + \sqrt{(\varepsilon - \varepsilon_0)^2 - 4V_c^2})^2}{(|\varepsilon - \varepsilon_0| + \sqrt{(\varepsilon - \varepsilon_0)^2 - 4V_c^2})^2 + \Gamma^2}, \quad (23)$$

for $|\varepsilon| > 2V_c$. This result explains the smooth tails seen in Fig. 3 when $|\varepsilon - \varepsilon_0|/\Gamma > 2$.

The conductance undergoes a bifurcation at $\alpha = 1/4$ ($|\varepsilon - \varepsilon_0| = 2V_c$), and there are not fixed points when $\alpha > 1/4$, namely $|\varepsilon - \varepsilon_0| < 2V_c$. Consequently, minute variations of the Fermi energy result in a dramatic change in the conductance of the QW, as it can be concluded from the lower panel of Fig. 3.

IV. SUMMARY

In this work, we studied the conductance at zero temperature of a side QD array attached to a QW. For a uniform QD array we found that the system develops an oscillating band with N antiresonances and $N - 1$ resonances arising from the hybridization of the quasibound levels of the QDs and the coupling to the QW. The positions of the antiresonances correspond exactly to the electronic spectrum of the isolated QD array. This property could be used to measure the energy spectrum of the N QD array. It should be stressed that the particular setup we suggested allows us to control the energy and

the width of the antiresonances in an independent fashion. When the number of attached QDs is large, a rich phenomenology appears for different values of the Fermi energy. When the Fermi energy lies far from the center of the QW band ($|\varepsilon - \varepsilon_0| > 2V_c$), the conductance presents regular and smooth behavior. However, the conductance strongly fluctuates close to the center of the QW band ($|\varepsilon - \varepsilon_0| < 2V_c$). These results pose a question about the relevance of the bifurcation at $|\varepsilon - \varepsilon_0| = 2V_c$ in actual experiments. Finally, we found an odd-even parity behavior of the conductance when the Fermi energy lies in center of the band. If the number of QDs in the array is even, perfect transmission takes place ($G = 2e^2/h$). On

the contrary, perfect reflection occurs when this number is odd ($G = 0$). This property arises from the intrinsic electronic properties of the QD array.

Acknowledgments

P. A. O. would like to thank financial support from Milenio ICM P99-135-F and FONDECYT under grant 1020269. Work in Madrid was supported by DGIMCyT (MAT2000-0734) and CAM (07N/0075/2001).

-
- ¹ D. Goldhaber-Gordon, H. Shtrikman, D. Mahalu, D. Abusch-Magder, U. Meirav, and M. A. Kastner, *Nature* (London) **391**, 156 (1998); D. Goldhaber-Gordon, J. Göres, M. A. Kastner, H. Shtrikman, and D. Mahalu, *Phys. Rev. Lett.* **81**, 5225 (1998).
 - ² S. M. Cronenwett, T. H. Oosterkamp and L. P. Kouwenhoven, *Science* **281**, 540 (1998).
 - ³ A. W. Holleitner, C. R. Decker, H. Qin, K. Ebert, and R. H. Blick, *Phys. Rev. Lett.* **87**, 256802 (2001)
 - ⁴ A. W. Holleitner, R. H. Blick, A. K. Huttel, K. Eber, J. P. Kotthaus, *Science* **297**, 70 (2002).
 - ⁵ W. Z. Shangguan, T. C. Au Yeung, Y. B. Yu, and C. H. Kam, *Phys. Rev. B* **63**, 235323 (2001).
 - ⁶ Akira Oguri, *Phys. Rev. B* **63**, 115305 (2001).
 - ⁷ Z. Y. Zeng and F. Claro, *Phys. Rev. B* **65**, 193405 (2002).
 - ⁸ B.-Y. Gu, *Phys. Rev. B* **51**, 16840 (1995).
 - ⁹ P. S. Deo and A. M. Jaynnavar, *Phys. Rev. B* **50**, 11629 (1994).
 - ¹⁰ Ji-Rong Shi Beng-Yuan Shu, *Phys. Rev. B* **55**, 4703 (1997).
 - ¹¹ H. S. Wall, *Analytic Theory of Continued Fractions* (AMS Chelsea Publishing, New York, 1967).